Optimal wavelength scale diffraction gratings for light trapping in solar cells

2012 J. Opt. 14 024012

(http://iopscience.iop.org/2040-8986/14/2/024012)

J. Opt. **14** (2012) 024012 (9pp) doi:10.1088/2040-8978/14/2/024012

Optimal wavelength scale diffraction gratings for light trapping in solar cells

Teck Kong Chong[1], Jonathan Wilson[2], Sudha Mokkapati[2] and Kylie R Catchpole[2]

[1] School of Electrical and Information Engineering, University of South Australia, Adelaide, South Australia 5001, Australia
[2] Centre for Sustainable Energy Systems, College of Engineering and Computer Science, The Australian National University, Canberra, ACT 0200, Australia

Received 25 August 2011, accepted for publication 15 November 2011
Published 12 January 2012
Online at stacks.iop.org/JOpt/14/024012

Abstract
Dielectric gratings are a promising method of achieving light trapping for thin crystalline silicon solar cells. In this paper, we systematically examine the potential performance of thin silicon solar cells with either silicon (Si) or titanium dioxide (TiO_2) gratings using numerical simulations. The square pyramid structure with silicon nitride coating provides the best light trapping among all the symmetric structures investigated, with 89% of the expected short circuit current density of the Lambertian case. For structures where the grating is at the rear of the cell, we show that the light trapping provided by the square pyramid and the checkerboard structure is almost identical. Introducing asymmetry into the grating structures can further improve their light trapping properties. An optimized Si skewed pyramid grating on the front surface of the solar cell results in a maximum short circuit current density, J_{sc}, of 33.4 mA cm^{-2}, which is 91% of the J_{sc} expected from an ideal Lambertian scatterer. An optimized Si skewed pyramid grating on the rear performs as well as a rear Lambertian scatterer and an optimized TiO_2 grating on the rear results in 84% of the J_{sc} expected from an optimized Si grating. The results show that submicron symmetric and skewed pyramids of Si or TiO_2 are a highly effective way of achieving light trapping in thin film solar cells. TiO_2 structures would have the additional advantage of not increasing recombination within the cell.

Keywords: light trapping, diffraction gratings, solar cells, photovoltaics

(Some figures may appear in colour only in the online journal)

1. Introduction

The cost of photovoltaic power remains relatively high due to the amount of silicon used in conventional wafer-based solar cells. Thin crystalline silicon cells are a promising candidate for future renewable energy applications because of the greatly reduced amount of pure silicon used as the active material, together with the stability of the film and the ease of processing of the cell, making it extremely suitable for mass production [1, 2]. Thin films are also attractive due to the potential for lower bulk recombination [3, 4] and the potential for increasing open circuit voltage (V_{oc}) if a high level of optical confinement can be achieved [4].

Crystalline silicon is an indirect bandgap material and therefore it has a low absorption coefficient, α, for light wavelengths in the near-infrared region, with the absorption length $1/\alpha$ increasing from 10 μm to about 3 mm in the wavelength range 800–1100 nm. However, there are 36% of photons with energies above the bandgap of Si in this wavelength range [5]. Thus, effective light confinement is essential for thin crystalline silicon solar cells.

There are many ways to enhance the photon absorption for wavelengths in the near-IR region. The standard approach for wafer-based cells is to use pyramid structures on a silicon surface which are usually several microns or more in size to trap light within the solar cell [6]. Features of this size can be understood using geometrical optics, but such large

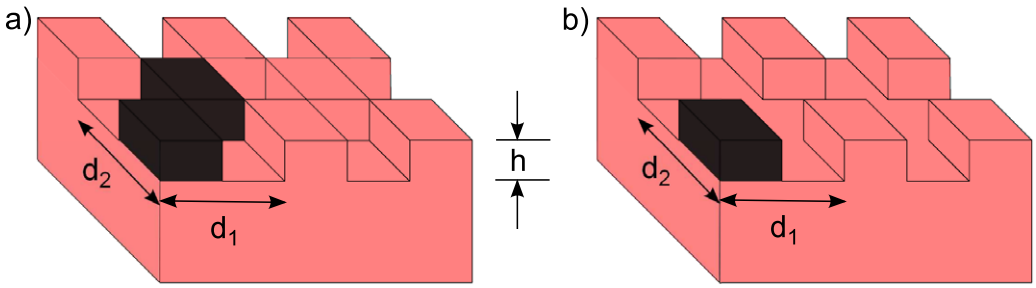

Figure 1. Schematic diagram of checkerboard (a) and square pillar structure (b).

features are not suitable for a thin film cell which may have a total thickness of only a few microns. Diffractive structures can also be used to increase the equivalent optical path length [7] and distributed Bragg reflectors (DBRs) can be used to reflect the light back into the substrates [8]. However, only a few investigations of diffractive structures for solar cell applications have been done to date. Feng *et al* investigated design optimization of a combined diffractive/DBR light trapping structure [7]. Morf *et al* have investigated groove gratings as summarized in [9], while Llopis and Tobias studied the effects of feature size for triangular grooves [10] and Abouelsaood *et al* have investigated the shape and size dependence of the anti-reflective and light trapping performance of triangular and rectangular grooves [11]. Meanwhile, Sai *et al* have investigated the light trapping effect of submicron surface textures in crystalline solar cell [12]. Some numerical studies have been done by Mellor *et al* as summarized in [13]. Kroll *et al*, on the other hand, have investigated numerically the application of dielectric diffractive structures in solar cells [14]. Clearly, up until now only particular structures of interest have been studied and no comparison of a wide range of structures has been done.

The number and the direction of the propagation of diffracted orders depend on the period of the grating and the wavelength of the light. The grating diffraction equation is

$$n_1 \sin\theta_1 = n_2 \sin\theta_2 = \frac{m\lambda}{d} \qquad (1)$$

where n_1 and n_2 are the refractive index of air and silicon, respectively, θ_1 and θ_2 are the angles of propagation in air and silicon, m is the diffracted order, λ is the wavelength and d is the grating period. For light trapping, incident light needs to be coupled to diffraction orders propagating outside the escape cone of Si. For very small periods ($d \ll \lambda$) higher-order diffraction modes do not exist in Si, so small period gratings cannot provide light trapping. While there are conceptual models available for optimization of very large period gratings [15], and for particular structures such as rectangular grooves [16] and pillars [17], there is no general conceptual model for gratings with wavelength scale periodicity. Diffraction gratings with wavelength scale features need to be optimized using numerical studies and this optimization is the subject of this study.

In this paper, we examine the behavior and the potential performance of diffractive structures constructed from either silicon or titanium dioxide (TiO_2) on silicon thin films. TiO_2 gratings were studied because they allow a surface texture to be applied to a finished cell, avoiding the reduction in material quality and increase in surface recombination associated with texturing the active Si region [18]. The potential short circuit current density (J_{sc}) for the optimized structures is compared against the planar cell and a cell with an ideal Lambertian scatterer. A Lambertian scatterer is a perfectly randomizing surface. Absorption in Si with a Lambertian scatterer is calculated following the approach of Goetzberger [19]. Regardless of the material used to construct the grating, the effective thickness of the cell is fixed at 3 μm, where the effective thickness is the height of a planar structure of equivalent volume per unit area.

2. Method

We investigate two single-period structures, rectangular grooves and sinusoidal grooves. The rest of the structures are biperiodic and included pillars, pyramids, grid and checkerboard structures. The grid structures are the inverse of pillar gratings. For biperiodic structures, both periods were varied independently of each other. The periods, d_1 and d_2, and the height, h, of the structures were varied between 0.2 and 1.2 μm for all the structures. However, the step size of the periods and height was set at either 0.05 or 0.1 μm. Figure 1 shows the schematic diagram of some of the biperiodic structures. The structure on the left (a) is a checkerboard structure and the square pillar structure (b) is on the right. The unit cell used to define the periods is also indicated in the diagram (shaded gratings) by the period (d_1 or d_2) and height, h.

The height of a pyramid structure is constructed by stacking a number of strata (staircase-like layers). As such, different potentials J_{sc} that can be generated by a pyramid structure could be significantly affected by the number of strata due to different light diffraction properties. As a result, convergence tests of the number of strata for pyramid structures were performed. It was found that the J_{sc} did not change provided that the number of strata was 15 or greater (with reference to the maximum diffraction order, m, considered in this study). As a result this number has been used for our study and it is valid for the ranges of height for pyramid structures mentioned in this paper.

Table 1. The potential short circuit current densities for all the model structures including comparable reference structures; planar and Lambertian model. The effective thickness of the Si film is fixed at 3 μm.

Name of structure	J_{sc} (mA cm^{-2})	Optimized parameters		
Reference structures				
		d_1 (nm)	h (nm)	
Planar	13.2	N.A	N.A	
Ideal Lambertian	36.8	N.A	N.A	
Uniperiodic (1D) structure				
		d_1 (nm)	h (nm)	
Rectangular groove	20.8	600	1000	
Sinusoidal groove	25.8	600	800	
Biperiodic (2D) structure				
		d_1 (nm)	d_2 (nm)	h (nm)
Square pillars	26.0	600	600	600
Rectangular pillars	25.6	700	600	600
Square pyramid	31.6	800	800	800
Rectangular pyramid	29.8	800	1200	1000
Checkerboard	26.0	800	800	1000
Square grid	23.3	600	600	1000
Rectangular grid	21.7	600	400	600

The optimum combination of periods, d_1 and d_2, and height, h, for each of the grating structures was found by weighted integration of each combination (d_1, d_2 and h) over the full wavelength range (400–1100 nm). The set of simulations was performed twice: once with a structure entirely made of silicon and once with an active planar layer consisting of silicon and a grating structure of TiO_2. Absorption within the TiO_2 was neglected for this study. There is no back reflector used for all model structures studied in this paper, including the reference structures.

The maximum diffraction order m can be found from the condition $\sin\theta < 1$ applied to equation (1). Although m can be as large as 14, it was found that about half of the orders ($m = 8$–14) have very little effect on the overall results. This is because these higher orders are only present at short wavelengths where silicon is strongly absorbing and light trapping is not important. However, the higher orders take up a lot of memory. So, the maximum m was set to 7 for computational efficiency purposes.

In order to find the power coupled into each diffracted order we used rigorous coupled wave analysis (RCWA) using GD-Calc under the Matlab environment. In this work, RCWA is used to calculate the diffraction efficiencies for all the structures. The absorption can then be calculated as

$$A = 1 - \left[\sum_m R_m + \sum_m T_m\right] \qquad (2)$$

where R_m and T_m are the reflected and transmitted efficiencies of the mth diffracted order. The potential short circuit current density was then calculated by integrating the absorption multiplied by the photon flux per unit wavelength over the full spectrum of 400–1100 nm. The coherence length of sunlight is around 1 μm and is similar to our cell thickness. The separation of the different parts of the spectrum by the grating will also tend to increase the coherence length. Therefore it is reasonable to include coherent interactions between the front and back of the cell into account.

In order to understand the separate effects of light trapping and minimizing front surface reflection, the following cases are analyzed: (1) silicon solar cells with silicon diffraction gratings without an anti-reflection (AR) coating, (2) silicon solar cells with silicon diffraction gratings with 70 nm SiN AR coating, (3) silicon solar cells with titanium dioxide (TiO_2) grating and (4) silicon solar cells with titanium dioxide (TiO_2) grating on the rear surface and a front AR coating.

3. Results and discussion

3.1. Si gratings

The potential short circuit current densities for all the model structures including a reference planar and Lambertian model are illustrated in table 1.

From table 1, we can see that, for uniperiodic structures, the sinusoidal groove is the most promising structure. With a sinusoidal groove grating on the front surface of a 3 μm thick Si solar cell the J_{sc} increases by 95% to 25.8 mA cm^{-2}, compared to the planar case.

Since we are looking at diffraction gratings on the illuminated surface of the solar cell, the increase in J_{sc} is partly due to the anti-reflection effect and partly due to the light trapping effect. Figure 2 shows the absorptance in the solar cell as a function of wavelength for the optimal sinusoidal and rectangular grating on the front surface. Higher absorptance for the structure with the sinusoidal grating in the long wavelength region could be either due to better anti-reflection or better light trapping properties of the structure. The effects of the two mechanisms cannot be decoupled. However, in the short wavelength region, where Si is strongly absorbing, the higher (near-ideal) absorptance in the structure is entirely due to the anti-reflection property of the grating. Light trapping is not critical for this region of the spectrum as light has a very short absorption length. Since a diffraction grating with a sinusoidal profile results in a gradual change of refractive index compared to a rectangular groove grating, it provides better anti-reflection and hence larger J_{sc} compared to a rectangular structure.

From table 1, we can see that biperiodic structures in general perform better than single-period structures. Results presented in table 1 are the average J_{sc} expected for TE and TM polarized light. For non-symmetric biperiodic structures, such as rectangular pillars, rectangular pyramids, rectangular grids, etc, due to the non-symmetry of the structure periods, TE and TM polarized light result in slight performance differences. On the other hand, for a symmetric biperiodic structure ($d_1 = d_2$) TE and TM polarized light result in the same J_{sc}. However, from our simulations, single-period structures are more sensitive to the polarization of incident light and do not give equal performance for both TE and

Table 2. Effect of polarization on potential J_{sc} of different uniperiodic and biperiodic structures.

Name of structure	J_{sc} (mA cm^{-2})		
	TE polarizations	TM polarizations	Average TE and TM
Uniperiodic (1D) structure			
Rectangular groove	21.2	20.4	20.8
Sinusoidal groove	25.1	26.5	25.8
Biperiodic (2D) structure			
Square pillars	26.0	26.0	26.0
Rectangular pillars	25.9	25.3	25.6
Square pyramid	31.6	31.6	31.6
Rectangular pyramid	29.7	29.9	29.8
Checkerboard	26.0	26.0	26.0
Square grid	23.3	23.3	23.3
Rectangular grid	23.3	20.1	21.7

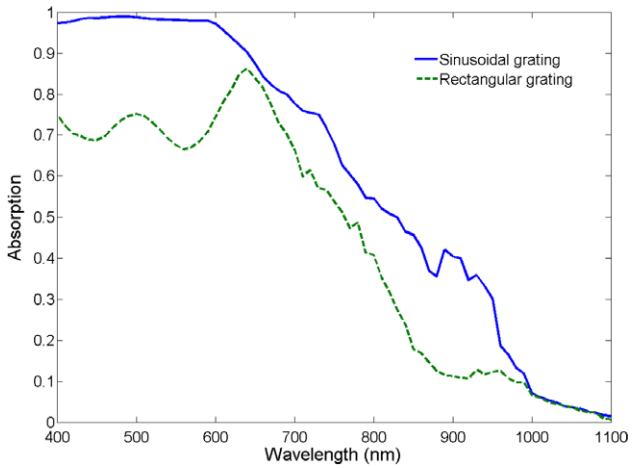

Figure 2. Comparison of absorption as a function of wavelength for sinusoidal and rectangular gratings on the front surface of a solar cell.

TM polarized light, resulting in lower average performance. Table 2 shows the effect of TE and TM polarization on symmetric and non-symmetric structures, with the average J_{sc} as shown in table 1 for comparison.

The periodicity of the grating also imposes constraints on the direction of the propagation of light in air and in Si. Only plane waves whose in-plane wavevectors satisfy the relation

$$\vec{k} = \vec{k}_0 + G_{m_1,m_2} \tag{3}$$

where $\vec{k}_0$ is the in-plane wavevector of incident light and G_{m_1,m_2} is the grating vector are supported. The wavevectors for the diffraction modes inside Si for single-period and biperiodic gratings are shown in wavevector space or k-space in figure 3. The allowed modes are separated from each other by $\frac{2\pi}{d}$. In addition, propagating modes in Si are bounded by a circle in k-space with radius $n\frac{2\pi}{\lambda}$, where λ is the wavelength of incident light in air and n is the refractive index of Si. As can be seen from the figure, with a biperiodic grating incident light can be coupled to more modes inside Si than a single-period grating, resulting in better performance. The same result was also found by Tobias *et al* [20], Yu *et al* [21] and Mellor *et al* [22].

The square pyramid produced the highest J_{sc} of 31.6 mA cm^{-2} among all the structures investigated, which corresponds to 139% enhancement with respect to the planar structure. Both checkerboard and square pillar structures resulted in the same J_{sc} of 26.0 mA cm^{-2}. We will see later, however, that the difference between these structures and the square pyramid structure is greatly decreased when an anti-reflection coating is included. From table 1, we also notice that biperiodic rectangular structures result in similar or lower J_{sc} compared to biperiodic square structures. So for the rest of the paper, we will only discuss biperiodic structures with equal periods, i.e. $d_1 = d_2$.

From figure 4, we can see that the difference in the performance of a square pyramid grating and the checkerboard or pillar grating is mainly in the wavelength range of 400–700 nm. While the structure with a pyramid grating has close to ideal absorption in this wavelength region, structures with checkerboard or pillar gratings result in lower absorption.

To investigate this further we integrated the short circuit current over two wavelength ranges: 400–700 and 700–1100 nm. Table 3 summarizes the results. In the short wavelength region there is 2.7 mA cm^{-2} difference in J_{sc} between the square pyramid structure and the square pillar structure, while there is 2.3 mA cm^{-2} difference in the long wavelength region. There is a larger difference between the checkerboard structure and the pyramid structure in the short wavelength region. In the wavelength range 400–700 nm, anti-reflection is the dominant effect in increasing the absorption in the cell, whereas in the range 700–1100 nm, both anti-reflection and light trapping play a role for structures on the front surface. The results therefore indicate that better anti-reflection is responsible for most of the difference between the three structures. Again, as in the case of single-period structures better anti-reflection properties for the pyramid grating can be attributed to a gradual change in refractive index from the apex to the base of the pyramids.

To further investigate the effect of anti-reflection on the results, a layer of 70 nm thick SiN anti-reflection coating was added to the structures to analyze the effect of AR in enhancing the photon absorption by the cells. Table 4 shows

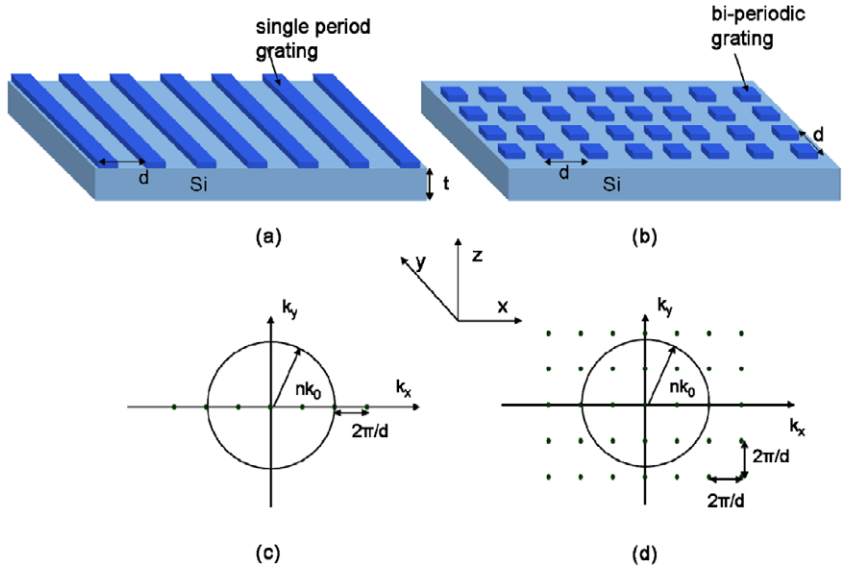

Figure 3. (a) Schematic of a single-period grating; (b) schematic of a biperiodic grating; (c) accessible diffraction modes inside Si with a single-period grating, represented in wavevector space and (d) accessible diffraction modes inside Si with a biperiodic grating, represented in wavevector space.

Table 3. The short circuit current density (J_{sc}) produced by the cells in different wavelength ranges.

	J_{sc} (mA cm^{-2}) for wavelength range	
Name of structures	400–700 nm	700–1100 nm
Planar	9.9	3.1
Square pyramid	18.4	13.2
Checkerboard	15.4	10.9
Square pillars	15.7	10.9

the results. Generally an improvement of about 2.5 mA cm^{-2} is achievable for pillar-type structures after a thin layer of SiN is added. This represents at least a 10% enhancement in short circuit current density

For checkerboard and pillar gratings, there is a substantial increase in the J_{sc} with the anti-reflection coating. For the square pyramid structure in our simulations, the reduction in reflection is not significant. This is because multiple reflections already occur due to the small facet angle, reducing the overall reflection and making the effect of the AR coating less important. As a result, the improvement in J_{sc} for pyramid structure with AR coating was not large. Nevertheless, it is extremely important to select an optimum thickness of AR for maximum benefit if large facet angles are used, since the effect of AR coating is significant for triangular groove or pyramid structures with facet angles larger than 55° [23].

3.2. *TiO_2 gratings*

While silicon gratings can be very effective in improving the absorptance in thin film cells, they can also lead to increased surface [24–26], emitter recombination [24] and bulk recombination [25, 26]. An alternative is to use a planar silicon cell with a grating of another material on the surface, avoiding this increased recombination. In the second part of this study, we investigate the enhancement in current achievable with titanium dioxide gratings on silicon substrates. We chose to study TiO_2 gratings as they can be fabricated using nano-imprinting, a cheap and large area patterning technique, and may also be able to provide surface passivation for Si [18]. The absorption within the TiO_2 was neglected for this study.

In general, J_{sc} produced by TiO_2 gratings on a silicon substrate exhibited the same trends as silicon gratings on a silicon substrate. Interestingly, although the refractive index of

Table 4. The J_{sc} results and optimized parameters for the best three structures.

			Optimized parameters	
Name of structures	Type of texturing	J_{sc} (mA cm^{-2})	d_1 (nm)	h (nm)
Square pyramid structure	Front surface	31.6	800	800
	Front surface + AR	32.7	800	1000
Checkerboard	Front surface	26.0	800	1000
	Front surface + AR	29.1	800	1000
Square pillars	Front surface	26.0	600	600
	Front surface + AR	28.6	600	200

Table 5. The potential short circuit current density for the model structures constructed from TiO_2 grating on silicon substrate with effective thickness of the Si substrate fixed at 3 μm.

Name of structure	J_{sc} (mA cm^{-2})	Optimized parameters	
Reference structure			
		d_1(nm)	h (nm)
Planar	13.2	N.A	N.A
Ideal Lambertian	36.8	N.A	N.A
Uniperiodic (1D) structure			
		d_1 (nm)	h (nm)
Rectangular groove	21.3	400	200
Sinusoidal groove	23.2	800	600
Biperiodic (2D) structure			
		d_1 (nm)	d_2 (nm)	h (nm)
Square pillars	24.4	600	600	400
Rectangular pillars	24.3	700	600	400
Square pyramid	28.2	750	750	900
Rectangular pyramid	27.8	800	1200	800
Checkerboard	25.4	800	800	400
Square grid	22.3	600	600	200
Rectangular grid	21.3	600	400	200

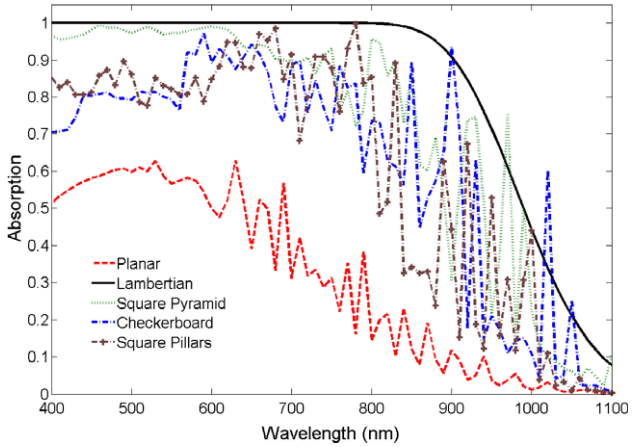

Figure 4. Absorption of the best three Si gratings on an Si substrate compared against absorption in planar Si and Si with Lambertian scatterer.

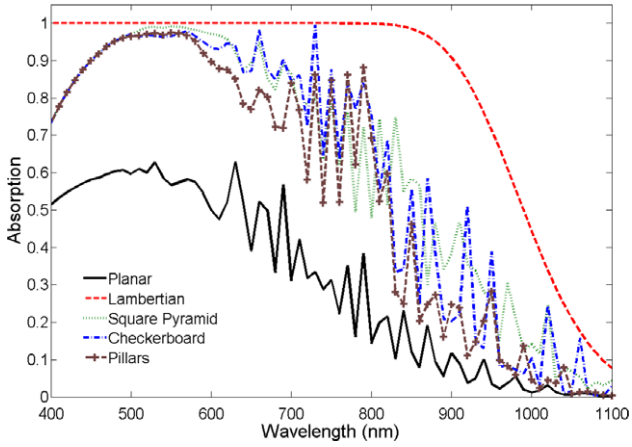

Figure 5. Absorption in a 3 μm thick planar Si layer and Si layer with a Lambertian scatterer or TiO_2 gratings on the rear. The front surface of Si is coated with 70 nm SiN for anti-reflection.

TiO_2 is significantly lower than that of silicon, the J_{sc} values predicted are only slightly lower. A sinusoidal grating remains the best uniperiodic structure with 23.2 mA cm^{-2} compared to 13.2 mA cm^{-2} for a planar structure. For biperiodic structures, a square pyramid remains the best structure with J_{sc} of 28.2 mA cm^{-2} followed by a checkerboard with J_{sc} of 25.4 mA cm^{-2} and pillars with J_{sc} of 24.3 mA cm^{-2}. The complete results, together with the optimum height, h, and period, d_1, are given in table 5.

The best three models (square pyramid, checkerboard and square pillars) were selected for further analysis. In order to investigate the potential of these gratings for different types of solar cells, a rear surface textured cell with and without a front AR coating was constructed. Figure 5 shows the result obtained for the case of a rear surface texture with front SiN AR coating (70 nm).

The potential short circuit current, J_{sc} for the three structures is shown in table 6. The table also illustrates the optimum period and height for each structure. We can see from table 6 that, for the cases with the texture on the rear and a front AR coating, the predicted J_{sc} for the checkerboard (26.1 mA cm^{-2}) and square pyramid structure (26.5 mA cm^{-2}) is very similar. Since the anti-reflection effect is the same in each case, this indicates, for structures on the rear of the cell, the light trapping provided by the square pyramid structure and the checkerboard structure is almost identical.

For diffraction gratings with wavelength scale periodicity, it has been proposed that introducing asymmetry into the

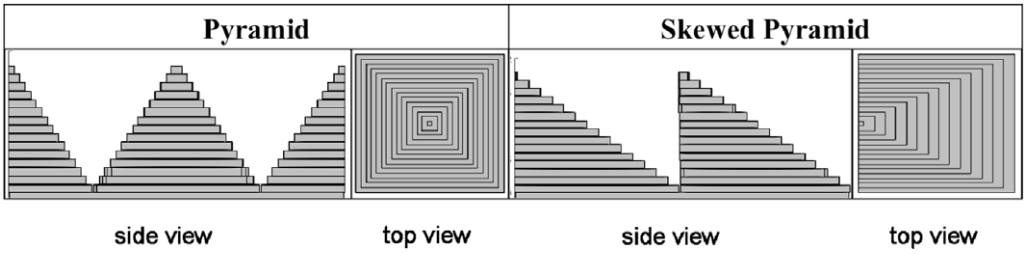

Figure 6. Side view and top view for the square and skewed pyramid structures.

Table 6. Summary of J_{sc} for front and rear TiO_2 surface textures, including rear surface textures with AR coating on the front side of the cell. All the cells have 3 μm thickness of Si.

			Optimized parameters		
Name of structures	Type of texturing	J_{sc} (mA cm^{-2})	d_1 (nm)	d_2 (nm)	h (nm)
Pyramid structure	Front surface	28.2	750	750	900
	Rear surface	16.9	850	850	600
	Rear surface + AR	26.5	850	850	600
Checkerboard	Front surface	25.4	800	800	400
	Rear surface	17.2	800	800	400
	Rear surface + AR	26.1	800	800	400
Square pillars	Front surface	24.3	600	600	400
	Rear surface	16.7	600	600	400
	Rear surface + AR	23.6	900	900	400

Table 7. A summary of J_{sc} for symmetric and skewed pyramid (Si or TiO_2) gratings on the front and rear of a 3 μm thick Si solar cell.

Symmetric structures				Asymmetric structures			
		Optimized parameters				Optimized parameters	
Type	J_{sc} (mA cm^{-2})	$d_1 = d_2$ (nm)	h (nm)	Type	J_{sc} (mA cm^{-2})	d (nm)	h (nm)
Si pyramids							
Pyramid front	31.6	800	800	Skewed pyramid front	33.4	750	750
Pyramid rear	21.5	850	350	Skewed pyramid rear	22.1	650	950
TiO_2 pyramids							
Pyramid front	28.2	750	900	Skewed pyramid front	28.9	700	750
Pyramid rear	16.9	850	600	Skewed pyramid rear	18.5	700	1000

grating structure can further improve its light trapping capabilities [21]. Having determined that pyramid gratings give the best performance of the symmetric structures studied, we investigated the effect of introducing asymmetry into the pyramid gratings to further improve the J_{sc} of the 3 μm thick solar cells. Figure 6 shows the side and top views of the skewed pyramid structures studied.

Table 7 summarizes the J_{sc} expected from a 3 μm thick Si solar cell with symmetric or skewed Si or TiO_2 pyramid gratings on the front or on the rear of the cell. For Si gratings on the front surface of the solar cell, the skewed pyramids result in a maximum J_{sc} of 33.4 mA cm^{-2}, which represents a 7% increase from J_{sc} of 31.6 mA cm^{-2} expected from the symmetric pyramid grating without AR coating. With optimized Si skewed pyramid gratings on the front side of the solar cell, the maximum expected J_{sc} is 86% of the J_{sc} expected from an ideal Lambertian scatterer. Figure 7 shows the absorptance in 3 μm thick Si with a Lambertian scatterer or a symmetric Si pyramid grating or a skewed Si pyramid grating on the front surface. Higher absorptance in the short wavelength region for the cell with a Lambertian scatterer shows that the difference between the performance of the cell with a Lambertian scatterer and a cell with an Si grating is mainly due to better anti-reflection from the Lambertian surface. For TiO_2 gratings on the front surface of the solar cell, the skewed pyramids result in 2.4% enhancement in J_{sc} compared to the symmetric pyramid structures, from 28.2 to 28.9 mA cm^{-2}. With optimized skewed TiO_2 gratings, the maximum expected J_{sc} is 79% of the J_{sc} expected from an ideal Lambertian scatterer.

Figure 8 shows the absorptance in 3 μm thick Si with a Lambertian scatterer, a symmetric Si pyramid grating or a skewed Si pyramid grating on the rear surface. We can see that Si gratings on the rear of the solar cell perform as well as a Lambertian scatterer on the rear. The maximum J_{sc} expected from a 3 μm thick Si solar cell with an ideal Lambertian

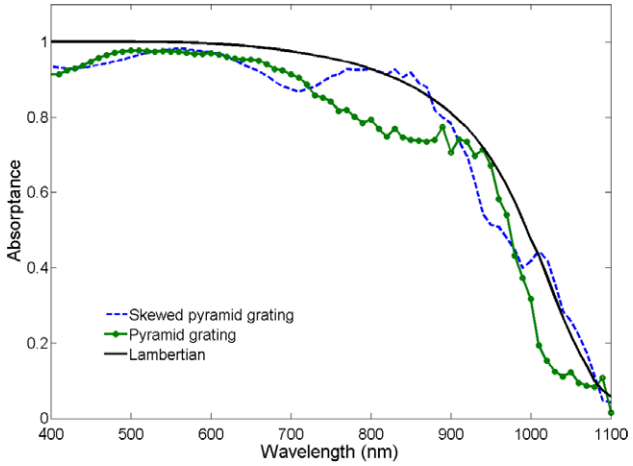

Figure 7. Absorptance as a function of wavelength in a 3 μm thick Si solar cell with a Lambertian scatterer, a symmetric Si pyramid grating or a skewed Si pyramid grating on the front surface.

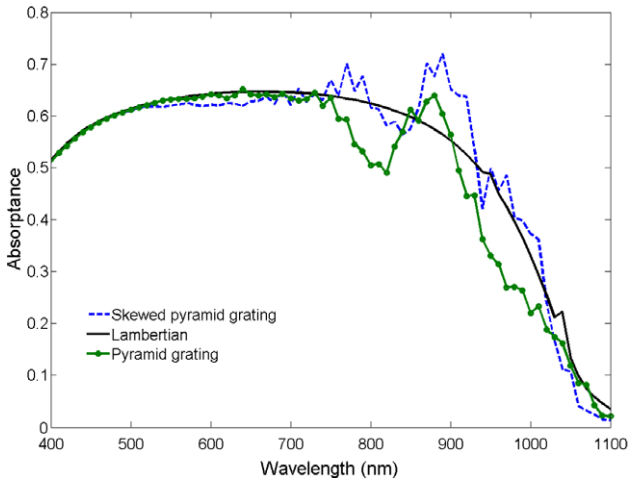

Figure 8. Absorptance as a function of wavelength in a 3 μm thick Si solar cell with a Lambertian scatterer, a symmetric Si pyramid grating or a skewed Si pyramid grating on the rear surface.

scatterer on the rear is 21.1 mA cm^{-2}. For gratings on the rear of the solar cell, the Si and TiO_2 skewed pyramids result in 3% and 9.5% enhancement, respectively, in J_{sc} compared to the symmetric pyramid structures. For optimized skewed pyramid gratings on the rear surface of the solar cell, the TiO_2 gratings result in 84% of the current expected from the Si gratings.

4. Conclusions

We have presented a numerical study of Si and TiO_2 diffraction gratings with wavelength scale periodicity for light trapping in 3 μm thick Si solar cells. Si gratings result in better performance compared to TiO_2 gratings because of higher refractive index contrast. For both materials, biperiodic gratings result in higher J_{sc} from the solar cell compared to single-period gratings. Of all the structures investigated, pyramid structures resulted in the highest J_{sc}. For gratings on the illuminated surface of the solar cell, both anti-reflection and light trapping effects lead to increased J_{sc}, while for gratings on the rear of the solar cell the J_{sc} enhancement is only due to light trapping.

Introducing asymmetry into the square pyramid structure further improves the performance of the biperiodic gratings. For skewed Si gratings on the front surface of the solar cell, a maximum J_{sc} of 33.4 mA cm^{-2} is expected, which is 91% of the current density expected with an ideal Lambertian scatterer. With an optimized TiO_2 skewed pyramid grating on the front surface, the maximum J_{sc} obtainable is 79% of that expected from an ideal Lambertian scatterer. For gratings on the rear surface of the solar cell, Si skewed pyramid gratings perform as well as a Lambertian surface and J_{sc} from the skewed TiO_2 pyramid grating is 84% of the maximum J_{sc} obtained using a skewed Si grating.

Acknowledgments

One of the authors (TKC) would like to thank CSES of the Australian National University for the opportunity given to explore this topic. We would like to thank the Australian Research Council and the Australian Solar Institute for financial support.

References

[1] Hamakawa Y 2004 *Thin-Film Solar Cells: Next Generation Photovoltaics and Its Applications* (Berlin: Springer) chapter 2, pp 15–39

[2] Nelson J 2003 *The Physics of Solar Cells* (London: Imperial College Press) chapter 8, pp 211–51

[3] Zeng L, Yi Y, Hong C, Liu J, Feng N, Duan X, Kimerling L C and Alamariu B A 2006 Efficiency enhancement in Si solar cells by textured photonic crystal back reflector *Appl. Phys. Lett.* **89** 111111

[4] Tiedje T, Yablonovitch E, Cody G D and Brooks B G 1984 Limiting efficiency of silicon solar cells *IEEE Trans. Electron Devices* **31** 711–6

[5] Bermel P, Luo C, Zeng L, Kimerling L C and Joannopoulos J D 2007 Improving thin-film crystalline silicon solar cell efficiencies with photonic crystals *Opt. Express* **15** 16986–7000

[6] Campbell P and Green M A 1987 Light trapping properties of pyramidally textured surfaces *J. Appl. Phys.* **62** 243

[7] Ning-Ning F, Michel J, Lirong Z, Jifeng L, Ching-Yin H, Kimerling L C and Xiaoman D 2007 Design of highly efficient light-trapping structures for thin-film crystalline silicon solar cells *IEEE Trans. Electron Devices* **54** 1926–33

[8] Johnson D C *et al* 2005 Advances in Bragg stack quantum well solar cells *Sol. Energy Mater. Sol. Cells* **87** 169–79

[9] Morf R H, Kiess H and Heine C 1997 Diffractive optics for solar cells *Diffractive Optics for Industrial and Commercial Applications* ed J Turunen and F Wyrowski (Berlin: Akademie) pp 361–89

[10] Llopis F and Tobías I 2005 Influence of texture feature size on the optical performance of silicon solar cells *Prog. Photovolt., Res. Appl.* **13** 27–36

[11] Abouelsaood A A, El-Naggar S A and Ghannam M Y 2002 Shape and size dependence of the anti-reflective and light-trapping action of periodic grooves *Prog. Photovolt., Res. Appl.* **10** 513–26

[12] Sai H, Kanamori Y, Arafune K, Ohshita Y and Yamaguchi M 2007 Light trapping effect of submicron surface textures in crystalline Si solar cells *Prog. Photovolt.* **15** 415–23

[13] Mellor A, Tobías I, Martí A and Luque A 2011 A numerical study of Bi-periodic binary diffraction gratings for solar cell applications *Sol. Energy Mater. Sol. Cells* **95** 3527–35
[14] Kroll M, Fahr S, Helgert C, Rockstuhl L, Lederer F and Pertsch T 2008 Employing dielectric diffractive structures in solar cells—a numerical study *Phys. Status Solidi* a **205** 2777–95
[15] Mokkapati S, Beck F J and Catchpole K R 2011 Analytical approach for design of blazed dielectric gratings for light trapping in solar cells *J. Phys. D: Appl. Phys.* **44** 055103
[16] Catchpole K R 2007 A conceptual model of the diffuse transmittance of lamellar diffraction gratings on solar cells *J. Appl. Phys.* **102** 013102
[17] Catchpole K R and Green M A 2007 A conceptual model of light coupling by pillar diffraction gratings *J. Appl. Phys.* **101** 063105
[18] Barbé J, Thomson A F, Wang E-C, McIntosh K and Catchpole K 2012 Nanoimprinted TiO_2 sol–gel passivating diffraction gratings for solar cell applications *Prog. Photovolt., Res. Appl.* at press
[19] Goetzberger A 1981 Optical confinement in thin Si solar cells by diffuse back reflectors *15th Photovoltaic Specialists Conf. (Kissimmee, FL)* pp 867–70
[20] Tobias I, Luque A and Marti A 2008 Light intensity enhancement by diffracting structures in solar cells *J. Appl. Phys.* **104** 134502
[21] Yu Z, Raman A and Fan S 2010 Fundamental limit of light trapping in grating structures *Opt. Express* **18** A366–80
[22] Mellor A, Tobias I, Marti A, Mendes M and Luque A 2011 Upper limits to absorption enhancement in thick solar cells using diffraction grating *Prog. Photovolt., Res. Appl.* **19** 676–8
[23] Gangopadhyay U, Dutta S K and Saha H 2008 Recent research trends in texturization and light trapping in silicon solar cells *Solar Cell Research Progress* ed J A Carson (New York: Nova Science Publisher Inc) pp 53–129
[24] Basore P A 1990 Numerical modeling of textured silicon solar cells using PC-1D *IEEE Trans. Electron Devices* **37** 337–43
[25] McCann M J, Catchpole K R, Weber K J and Blakers A W 2001 A review of thin-film crystalline silicon for solar cell applications. Part 1: native substrates *Sol. Energy Mater. Sol. Cells* **68** 135–72
[26] Rockstuhl C, Fahr S, Lederer F, Haug F-J, Soderstrom T, Nicolay S, Despeisse M and Ballif C 2011 Light absorption in textured thin film silicon solar cells: a simple scalar scattering approach versus rigorous simulation *Appl. Phys. Lett.* **98** 051102